PLASMA ETCHING OF GaAs SURFACE IN A PLANAR GAS DISCHARGE SYSTEM

B.G. SALAMOV [a] and T.G. MAMMADOV [b]

[a] *Physics Department, Faculty of Arts and Sciences, Gazi University,*
Beşevler 06500 Ankara, Turkey
[b] *Azerbaijan National Academy of Sciences, Institute of Physics,*
AZ-1143 Baku, Azerbaijan

This paper analyses the surface behaviour of etched a large-diameter GaAs plate realized by recording the spatial distribution of the gas discharge light emission (DLE) in a planar gas discharge system (PGDS) in ambient air and room temperature. The etching depth is measured by surface profilers as a function of a gap spacing and gas pressure. The analysis of the surface homogeneity is determined by fractal dimension of the gas DLE when a limiting current is passed through a discharge cell. The effect on the roughness of the GaAs surface through the plasmachemical processes at appropriate set of experimental parameters was established. The surface images of the etched GaAs are analysed using both the profile and spatial distribution DLE intensity data showing the surface inhomogeneity in the GaAs plate. It is quantitatively concluded that plasma etching at certain experimental condition can cause an improvement in surface structure of GaAs plate and spatial distribution DLE in a PGDS. The results obtained in this work suggest that a PGDS can be an efficient, alternative plasma source for general surface processing, because they can provide nonthermal discharges also near atmospheric pressures and thereby eliminate the need of costly vacuum systems.

1. INTRODUCTION

The III-V compound semiconductors, such as GaAs and InP, have been long recognised for their potential applications in high speed electronic and optoelectronic circuits. The technology of reducing the negative effects of poor surface and interface is referred to as plasmachemical processes, the objective of which is to stabilise the properties of the surface so that it becomes immune to exposure of the device to operating ambient [1]. Plasmachemical processes have proved to be very useful methods for cleaning, etching, or material deposition on surfaces and have enabled the production of new and advanced materials for a variety of technical applications [2-4]. In all surface-processing techniques using plasmas, activated species (e.g., ions, electrons, photons, radicals and metastables from the working or background gas) [4,5] are generated within the plasma which then undergo chemical and physical reactions with the surface material. Examples are etching of Si and SiO_2 with X (where X = F or Cl) from NX_3, CX_4, C_2X_6, or C_3X_8 in the semiconductor industry, degreasing of metal parts by $O(^3P)$ and $O(^1D)$, $O_2(^1\Delta)$, and O_3 in the metal industry [6] or coating of materials with polymers or other materials in various industry branches [3,7,8].

A planar gas discharge system (PGDS) with a semiconducting cathode has found numerous applications in the last decade, especially in the registration of IR images. High speed photography, non-silver image formation and devices for rapid visualization of electrical and structural defects in semiconductors are the other interesting applications of these systems [9-11]. It is known [11] that if one of the electrodes is made in the form of a GaAs plate with a resistivity greater than 10^6 Ωcm in a PGDS cell, the gas discharge current can be distributed over the whole area of the electrodes causing a gas DLE. The uniformity of the DLE depends on the resistivity distribution of the GaAs plate, and the light emission intensity is proportional to the discharge current. Local changes in the resistivity of the GaAs plate leads to local changes in the current and the gas DLE. The current and DLE intensity depend on the local parameters of the GaAs plate, and therefore inhomogeneities in the GaAs plate are visualized in the form of irregularities in the DLE.

The presence of many electronically active defect states results in poorer device performance and reliability. Therefore, preparation of surface with acceptable levels of electronically active defects is essential for proper functioning of many devices. Unfortunately, the fundamental knowledge of the surfaces has been very limited and the research of reducing the negative effects of poor surface and interface, for Si and III-V compound semiconductors, has been primarily based on empirical techniques [1]. It is recognized that the development of GaAs semiconductor technology is directly related to the surface properties of GaAs. Hence, the control and precision in surface treatment such as the cleaning and etching processes is becoming increasingly critical in devices occur [12]. The methods for visualization the surface homogeneities of GaAs plates of large diameter are of great interest for the electronics industry and laboratory studies [11]. Therefore, any relevant evaluation of the homogeneity of

131, H.Javid ave, AZ-1143, Baku
ANAS, Institute of Physics
E-mail: jophphysics@gmail.com

semiconductor requires description of the spatial distribution both of surface roughness and of structural defects. Moreover, in addition to provide an image of the GaAs plate, analysis of this image is important to confirm the homogeneities spatially in a PGDS with a semiconductor cathode.

In contrast to discharge devices with metal electrodes, the voltage drop in the discharge gap of a laterally extended semiconductor gas discharge cell is localized. These cells are more stable against the current filamentation because there exists negative feedback caused by the appearance of tangential components of the electric field in the case of imposing on the system an inhomogeneous fluctuation of j [13,14]. As a result, instabilities of the "fluctuation" type may not occur. Mechanisms for this include distortion of the field by the space charge, gas heating, or the dependence of the secondary electron emission factor γ, on the ion energy and hence on the strength of the field at the semiconductor. The presence of a resistive electrode also affects the development of instabilities of the ionization-overheating type. It was shown in [15] that in a PGDS with the Townsend discharge, the resistive electrode reduces the growth rate of the instability and under certain conditions may suppress it completely.

The uniform DLE over the whole electrode area was observed with currents of more than 100μA. An advantage of PGDS over low pressure gas discharge (i.e., rf or microwave in a pressure range of a few *m*Torr to a few Torr) and dielectric barrier discharge (i.e., in a pressure range 500-1500mbar) is the nonthermal behavior at high gas pressures and uniform (i.e., without filamentary) discharge mode. In most cases, it is desirable or even necessary to use nonthermal plasmas, because high gas temperatures can destroy the sample. Therefore, at a constant gap spacing (10-100μm) and a wide range of the gas pressure (20-700 Torr), even for critical electrical field strength ($E \cong 4\times10^4 V/cm$) and current densities ($j \cong 10^{-4}$ A/cm^2) values the discharge in a PGDS could be still rather uniform. Filamentation can cause distortion in the GaAs surface, leading to nonuniform processing of the surface. Therefore, the local changes in the surface irregularities of the GaAs plate lead to local changes in the current and the gas DLE. Therefore, nonuniform processing of the GaAs surface are visualized in the form of irregularities in the DLE. In a previous publication [16], we reported fractal dimension analysis as an alternative method to identify inhomogeneities in the semiconductor plate with large-diameter. This paper deals with etching of semiconductor material using a (near)-atmospheric non-thermal plasma source for general surface processing and thereby eliminate the need of costly vacuum systems. Moreover, one can determine surface irregularities in the large diameter semiconductor plates by the fractal dimension method.

2. EXPERIMENTAL

A schematic diagram of the experimental set-up and a PGDS equipped with a proximity focused image intensifier coupled to the charge coupled device (CCD) is shown in fig.1. A Cr-compensated GaAs ($\rho \sim 10^7 \Omega cm$) plate [17] was used as a semiconductor cathode. The diameter and the thickness of the plate were 30mm and 1mm, respectively. On the illuminated side of the GaAs, a transparent conducting vacuum-evaporated Ni-layer was coated. The anode was a disc of glass (of 30mm diameter and 2mm thickness) coated with a thin layer of transparent conductor SnO$_2$. The GaAs plates were selected from a number usually employed in a PGDS. Even after grinding and polishing the surface were not subjected to chemical etching: i.e., there was a strongly disturbed surface layer on the GaAs plate.

Gallium arsenide is a direct semiconductor with a band gap of 1.42eV at room temperature. When the radiation is absorbed, electrons are excited and perform transitions from the valence band to the conduction band. This internal photoeffect lowers the resistivity of the material. The light of an incandescent lamp with an Si-filter in front illuminates the cathode uniformly. The discharge can burn on a circular-shaped area with a diameter of 20mm. In the following, this area is often referred to as the active area. The DLE can be observed through the SnO$_2$ layer and the glass plate (fig.1). To ensure spatial homogeneous illumination, a homogeneous beam was prepared by a simple optical arrangement. The maximum illumination intensity is around 10^{-4} Wcm^{-2}.

The discharge current is measured as the voltage drop at the serial resistor $R=100\Omega$. This voltage drop is negligible in comparison with the applied high voltage. Therefore, the voltage at the electrodes of the PGDS is virtually equal to the applied voltage. The spatial distribution of the current density in the active area cannot be measured directly but it is proportional to the light density emitted by the discharge [9,19]. Therefore, measurements of the spatial distribution of DLE give also information about the corresponding behaviour of the current. Moreover, it is necessary to have in mind that the semiconductor plate does not act like a usual load resistor, but like a spatially distributed resistive layer. Due to this fact a spatially inhomogeneous IR light distribution projected on the semiconductor cathode will cause an equivalent modulated spatial resistivity distribution in the semiconductor. In other words, this means that the local resistivity of the semiconductor will have the lowest value where the radiation density has its highest value.

The discharge gap of the cell was filled with ambient air and the measurements were carried out at room temperature. The size of the discharge gap, d (80μm) and the residual gas pressure, p (100 Torr), were chosen to ensure a sufficiently bright DLE [18]. A voltage of up to 2,5kV was applied to the electrodes of the cell. DLE over the whole electrode area was observed with currents of more than 100μA.
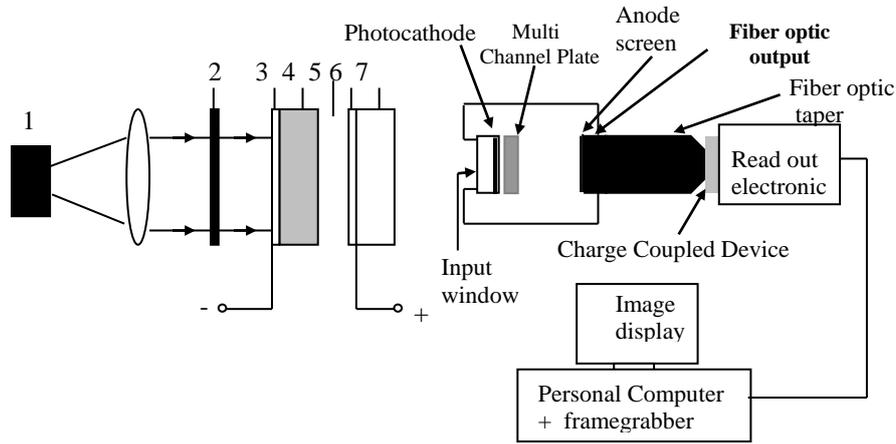
Fig. 1. Experimental setup and a PGDS equipped with a proximity focused image intensifier coupled to the CCD.
Numbers indicate: 1-light source; 2-Si filter; 3-transparent Ni-layer; 4-GaAs plate; 5-gas discharge gap;
6-planar transparent SnO_2 conductor; 7-flat glass disc.

In a PGDS cell the discharge gas does not distort the distribution of the current density in the GaAs plate.The assessment of the image formation was then based on analysis of the DLE (330–460nm), recorded through a transparent anode with spatial resolution via the corresponding light emission [19]. The minimum radiation energy density detected was $8x10^3 J/cm^2$. Under stationary conditions of image conversion, the spatial resolution of the device, R, was $\approx$10 lines per millimetre. With a diameter of the active part of the device of the order of 20mm. The emitted gas DLE is registered by an intensified CCD camera. The computer control and GPIB image transfer are integrated in the software to full automation of the measurement and calculation sequence. After the reference image has been recorded, the camera is focused onto the GaAs surface and a DLE image is recorded.

The two-dimensional (2D) image of a GaAs surface in a PGDS cell are presented in fig. 2a and fig. 2b. As it can be seen in fig.2, the dark regions are distributed on the light background. The dark regions correspond to a low discharge current, and hence to a high resistivity of the GaAs plate. Thus, the resistance inhomogeneities transform to DLE inhomogeneities [20]. If the conductance inhomogeneity is due to fluctuations in the number of the dislocations centers, it is possible to visualize the distribution of the dislocations centers (for more detailed information, see references [11,21]). The surface profilers and fractal analysis were carried out to characterize the surface state of GaAs plate after plasma etching, in order to establish the changes in surface roughness. After the etching process, the GaAs plate is analyzed for the etching depth using a 3-D surface profiler (Zygo, New View 5000).
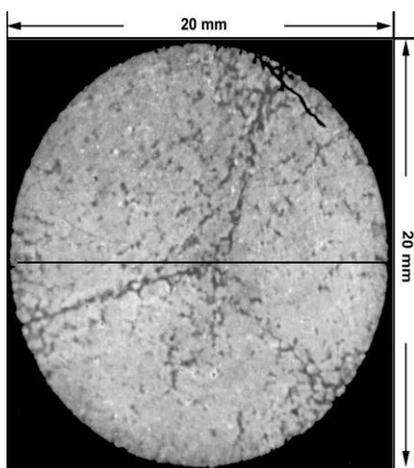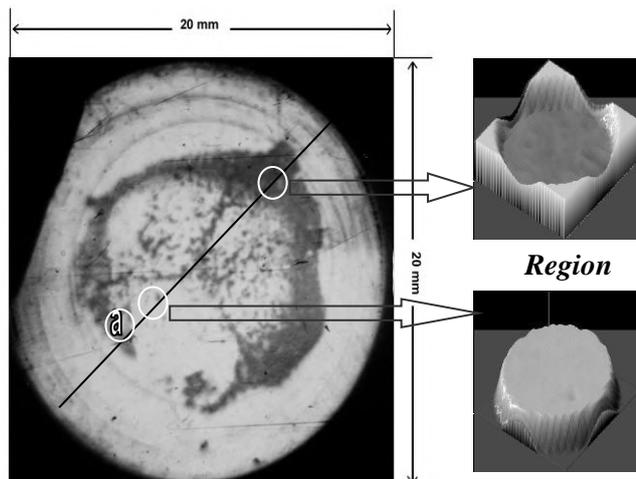
Fig. 2a *Fig. 2b*

Fig. 2. The (a) untreated and (b) treated 2D images of the GaAs surface in a PGDS cell. In Fig.2b signs (a), (b) indicates some examples of the plasma etching (i.e. distortion) and (c) smooth surface regions along the profile line, respectively.

A clear graphical representation of the results was obtained by using a discrete set of amplitudes of DLE intensity to smooth out approximating surfaces that passed through all the experimental points. Three-dimensional (3D) charts of the distribution of the DLE intensity or amplitude-coordinate distributions could represent the final results. The possibilities of the visualization have been evaluated, i.e., a local change in surface inhomogeneity is determined by a local change in DLE intensity.

3. RESULTS AND DISCUSSION

In semiconductor technology, it is revealed that the surface roughness causes a significant degradation of gate breakdown field strength and channel mobility [18,22,23], since a high surface recombination velocity of non-equilibrium carriers in the semiconductor is ensured in present a PGDS. Studies of the characteristics of such devices showed that they are strongly affected by the quality of the semiconductor electrode. This can be observed in part when uniform illumination of a semiconductor gives rise to a nonuniform pattern of the DLE.

In a PGDS cell a spatially inhomogeneous IR light distribution projected on the surface of the GaAs plate will cause an equivalent modulated spatial resistivity distribution in the GaAs plate. Relating to

different experimental conditions of the same semiconductor, 2D images have been obtained as in fig. 2a. and fig. 2b. While fig. 2a. gives a homogenous spatial appearance owing to the similar lightness, fig. 2b. has light and dark regions compared with fig. 2a. Effects of charge particles bombardment as a reasonable result of plasma-chemical processes are mostly seen as a C - shaped dark area with the surface distortions in fig.2b. Meanwhile some local distortions take place near the center of GaAs plate. Later, these distortions will be proved as the main cause of surface irregularities of the GaAs plate, quantitatively. In fig.2b. signs (a), (b) and (c) indicate some examples of the plasma-chemical etched and smooth regions along the profile line, respectively.

Magnified three-dimensional 3D forms of (b) and (c) regions indicate surface irregularities and smooth parts of the semiconductor material with respect to the DLE intensities. These images will be discussed later. To determine the light and dark regions of 2D images of the semiconductor surface effectively, fig.2a. and fig.2b. have been transformed into 3D form (fig.3a and fig.3b). As seen in fig.3a. and fig.3b, the DLE intensity has been given by a 3D GaAs surface pattern to identify the differences in the intensity values between the 2D images in fig. 2a. and fig. 2b.
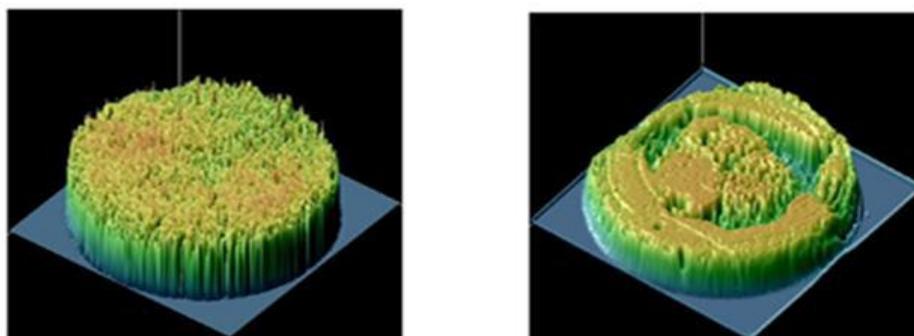
Fig. 3. The (a) untreated and (b) treated 3D surface patterns in a PGDS with a GaAs plate. The plate thickness was 1mm, the diameter was 30mm, the discharge gap width was 80μm, the applied voltage 800V, the air pressure was 100 Torr and the current was 100μA.
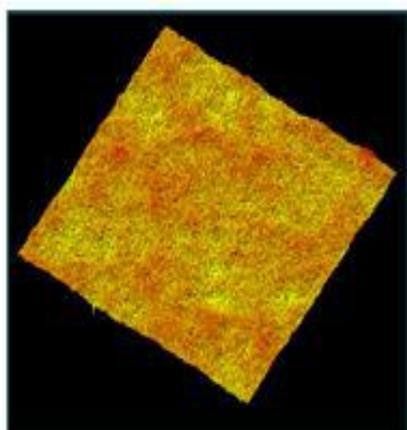
Fig.4a. 3D surface pattern of untreated region in fig.2a on the GaAs plate (2mm x 2mm) in a PGDS.

It is obvious that fig.3a differs from fig.3b in its emission intensity values and gives a homogenous spatial appearance owing to the similar DLE intensity distribution [16]. However, fig.3b. has an inhomogenous structure as a result of the very changeable emission intensity distribution as a qualitative feature. At this point, it is interesting that if fig.3a is compared with the 3D form of the region (c) in fig.2b, the DLE intensities in region (c) is seen to be smoother than that of fig.3a. We consider this event as a positive result of plasmachemical processes. The interaction between the gas mixture and semiconductor can generate smoother surfaces because of etching and desorption of the GaAs surface [24]. The effectiveness of desorption process is proportional to the densities of bombarding particles as well as the stream of desorpted particles leaving the

cathode surface. Meantime, the filamentation in a PGDS during a uniform illumination of the GaAs plate is since a higher conductivity in the cathode plate gives rise to more charging of the GaAs plate which leads to a higher gamma-coefficient on this plate [25,26]. This process in combination with ion bombardment might even explain the reproduction process of filamentation altogether. Filamentation enhances the desorpting of the GaAs surface at the corresponding (a) and (b) regions in fig.2 where the etched regions become deeper as the time progress (see fig.4b and fig.6b).

While increasing total current by illuminating the photosensitive GaAs plate or increasing the supply voltage, the density of the charged carrier in the discharge gap increases. This is accompanied by the formation of the net space charge in the discharge gap, and gradually the transition from the Townsend regime to the glow discharge regime takes place. Therefore, we want to mention that while passing from Townsend regime to the glow discharge space charge become important and the current flow through the gap is not homogeneous but constricted.
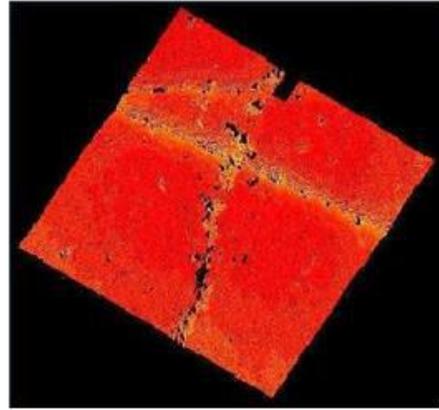
Fig. 4b. 3D smooth surface pattern of the same treated region in fig.4a on the GaAs plate (2*mm* x2*mm*) with the etched channels where the discharge current is higher than the critical and the etching depth increases to ~ 242*nm.* A surface profiler scan is shown in fig.4(c).
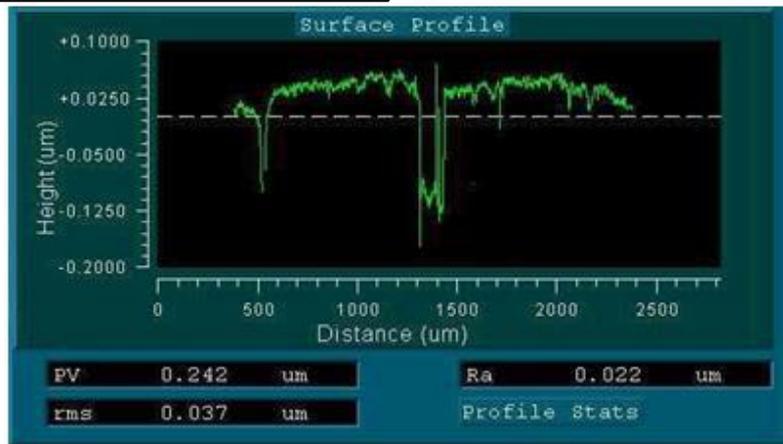
Fig.4(c). Surface profiler scan of etched region in Fig.4b on the GaAs surface caused by a PGDS at the discharge parameters above critical experimental conditions.

The discharge area spreads laterally by increasing the external applied voltage, while the current density stays nearly constant until finally, the discharge covers the whole electrode area. Therefore, due to the previous reason, surface profile reveals etched regions where the system pressure and gap produce a more uniform (without filamentary) discharge, resulting in smooth etched surface (region *c* in fig.2b); and regions where the discharge current is higher than the critical and the etching depth increases to ~242 nm in the etched channels on the surface (fig.4b). 3-D surface topography of untreated and treated region on the GaAs surface (2*mm*x2*mm*) is shown in fig.4a, b. After the etching process, the GaAs plate is analyzed for the etching depth using a 3-D surface profiler. A profiler scan of a typical distorted region caused by PGDS is shown in fig.4c.

Figure 5 shows the variation of the upper limits of current I_1 values (above which the filamentation starts), for three different illumination intensities of light ($L_1 > L_2 > L_3$), which lead to three different resistances of GaAs cathode (R_1, R_2, R_3). The following process resulting in a local increase in the current then occurs. Modulation of the bulk of the semiconductor cathode and a reduction in its resistance increase the current in the plasma, and also increase the intensity of the light emitted by the gas and the flux of the ionizing particles, which in turn reduce to an even greater degree the resistance of the semiconductor cathode in this range (for detailed information see [27]).

Possible explanations for the distortion include localized heating leading to vaporization, charge built-up, and release on or below the surface due to a small defect within the semiconductor material, or, most likely, due to charging which is thought to be the dominant damage mechanism in photoresist ashing [28,29]. Additionally, it is our observation that for all the pressure and gaps explored in this work the intensity of the filamentation can be adjusted, but in no instance was the discharge a homogeneous glow.
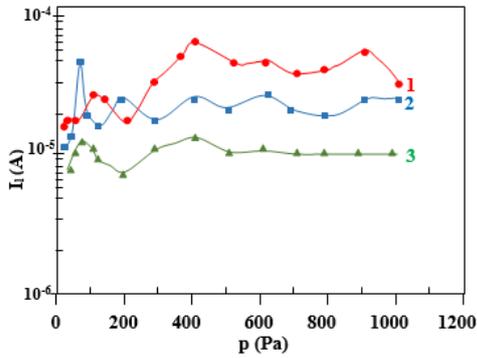
Fig.5. Dependence of the limiting current I_l, corresponding to the beginning of filamentation on pressure at the length of the discharge gap of $d = 30\mu$m. Curves 1, 2, 3 correspond to three different resistances $R_1 = 10^7\ \Omega$, $R_2 = 6\text{x}10^7\ \Omega$, $R_3 = 1.3\text{x}10^8\ \Omega$ of GaAs cathode.

Many earlier studies such as [24,30] utilized this kind of surface treatment technique to obtain convenient materials. In this manner, it will be noted later that fractal analysis method can be also considered as a qualitative analysis tool for earlier studies about this surface treatment technique. In addition to that, it should be also stated that distorted semiconductor regions such as (a) and (b) in fig.2b can be generated above critical experimental conditions (i.e., exposure time, gas pressure, p, discharge gap, d, feeding voltage, illumination intensity etc.). For present purposes, in this case, positive effects of plasma-chemical etching disappear and irregularities begin to increase on the whole surface of semiconductor.
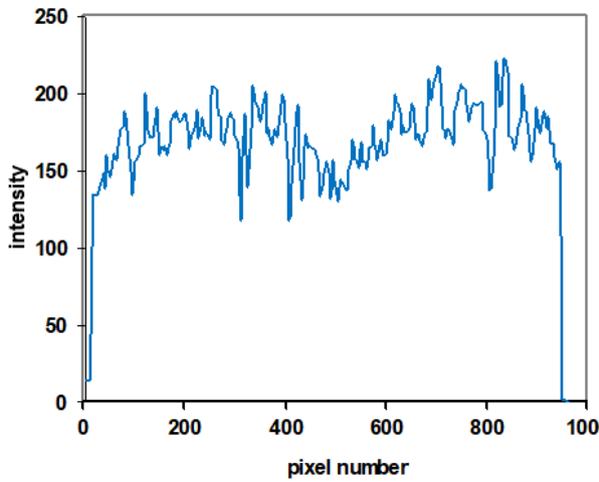
Fig. 6a
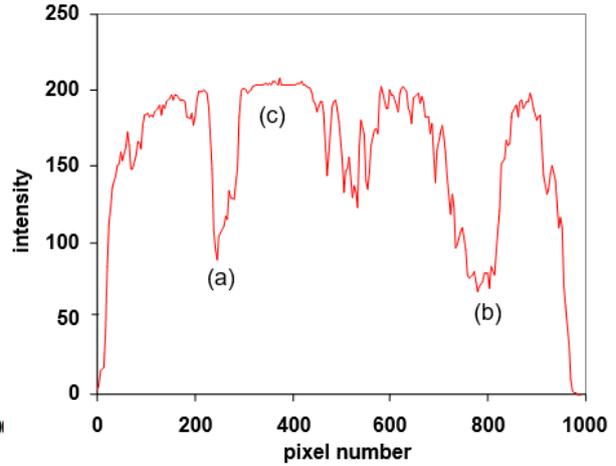
Fig. 6b

Fig. 6a, 6b. Variations of DLE intensities (i.e., gray levels) along the active semiconductor area diameter (20*mm*) of (a) untreated and (b) treated GaAs surface patterns. In fig.6b signs (a), (b) indicates some examples of the plasma etching regions along the profile line.

Fig. 6a and fig. 6b, which give a transformation of the DLE intensity into profile form in the active semiconductor area diameter as pixel number, clarify the differences between the 3D patterns more efficiently. The irregularities in the outer surface of the semiconductor plate are clearly visible, and these areas are indicated as two broken part grey-colored parts in the profile. The program at the chosen optimum conditions gave a better image quality. With the optimum value of the size of the discharge gap, d (80μm), and the gas pressure, p (100 Torr), the image contrast of the large semiconductor plates can be improved considerably with a reasonable improvement in the spatial resolution. In order to obtain more information, the images are constructed at various operating voltages for the same parts of the semiconductor plate. It is interesting to know that the all parts of the semiconductor plate are easily identified as a spatial pattern. In the present case, the differences between the maximal and minimal DLE intensity values among the pixels on the diameter of the semiconductor surface patterns are 104 and 180

for fig. 6a and fig. 6b, thereby indicating the untreated and treated surfaces respectively. However, one should eliminate the extreme plasma etched regions (i.e., signed with (a) and (b) in fig.2b), threshold pixel numbers of which are given by 224-294 for region (a), and 704-848 for region (b), to find out the accurate differences between the maximum and minimum DLE intensity values for the determination of positive effects of plasmachemical processes. For this aim, extreme plasma etched regions are indicated by grey-coloured curves in fig.6b. According to the dark curves, which represent the positive effects of etching in the optimal conditions, differences between the maximum and minimum light emission intensity values is found as 81 in the active area of the semiconductor. This result supports the above-mentioned idea that plasma etching improves the quality of a semiconductor surface and homogeneity of DLE, if the experimental conditions are determined appropriately, in the sense that the difference between the maximum and minimum DLE intensity values is

decreased from 104 to 81 for the same semiconductor plate.

A quantitative fractal dimension estimation has been carried out over the active area of DLE intensity to identifying the homogeneity in the spatial patterns given in fig. 3a and fig. 3b. To provide similar terminology between the DLE pattern and the analyze process, it should be stated that the DLE intensity values are referred to as grey levels and the term grid is used for a pixel. In this manner, fractal dimension analysis has been realized by calculating $L(R)$ for various R values inside a 960x960 pixel area with a

maximal 256 grey-levels for each pattern (for more detailed information see [16,31]). The fractal dimension of the coastline L is denoted by dimension D and can be found from the expression

$$D = -\frac{\log L(R)}{\log R} \qquad (1)$$

The value of $L(R)$ is calculated for each R (R is the grids size), and a log-log plot of $L(R)$ versus R is obtained. The slope of the least-square linear fit line will give $-D$.
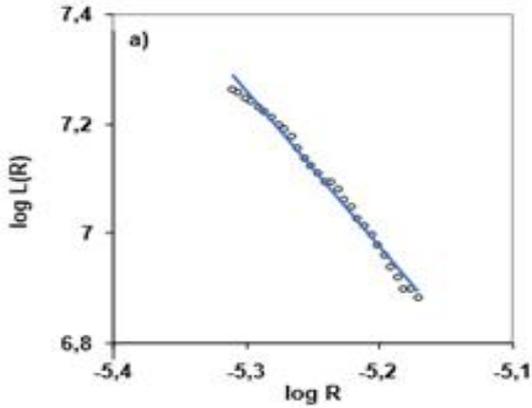
Fig. 7a
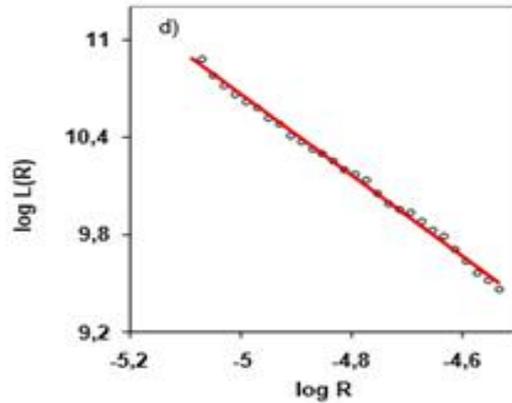
Fig. 7b
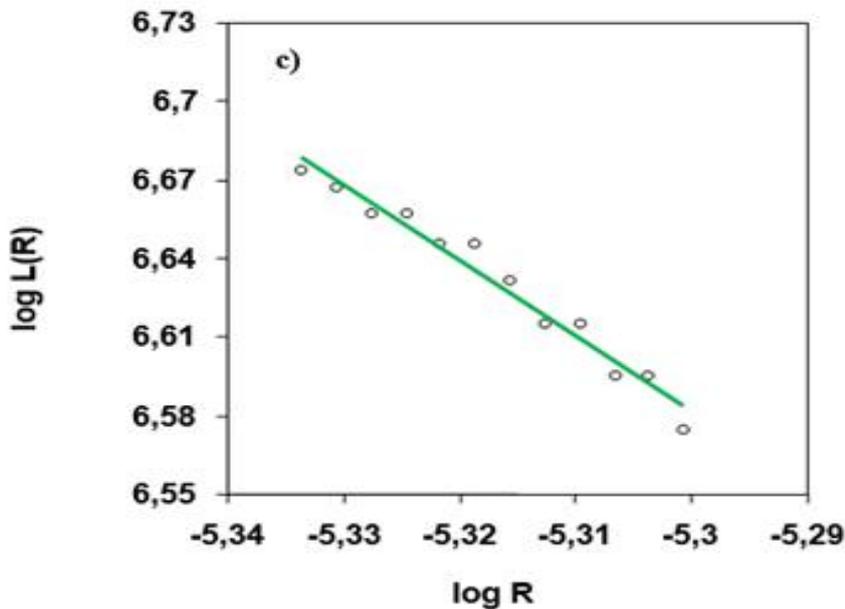
Fig.7c.

Fig. 7. The log-log plots of the DLE intensities of (a) untreated, (b) treated and (c) smooth GaAs surface patterns with the least square fit lines.

Fig. 7a, b and c present the results of analyses as log-log plots of each pattern with the least- squares linear fit lines. Dimension values have been extracted from the slopes of linear fit lines. According to the slopes in these plots, dimension values have been

found as $D=2.85$ and $D=2.52$ for fig. 3a and fig.3b, respectively. These dimension values provide precise knowledge for the homogeneity of the active area of the DLE surface pattern of the semiconductor as mentioned earlier, in the sense that high dimension

values indicate the excess of filled grids relating to their grey levels. Therefore, while the homogeneity rate of the DLE pattern seen in fig.3a is 2.85 (remember that the maximal value of *D* is 3), fig.3b gives an inhomogeneous appearance owing to its low *D* value. However, if one eliminates the extreme plasma etched regions, spatially in fig.3b, fractal dimension is found as *D*=2.89 from the log-log plot given in fig.7c. A quantitative fractal dimension estimation thereby confirm that plasma etching improves the quality of a semiconductor surface owing to higher dimension value than the dimension value of the untreated semiconductor. Moreover, the size and location of surface inhomogeneities in large-diameter semiconductor plates may be ascertained by this method. It can be considered that a local change in surface in the treated region is determined by a local change in DLE intensity. An analysis of the DLE pattern can be used to determine the effectiveness of visualization of the surface irregularities as a function of their structure [20]. The observed gas DLE patterns of the semiconductor plate make it possible to assert that the structural disturbance regions are those of accumulation of surface irregularities.

5. CONCLUSIONS

From the analyses on experimental findings, we could establish the etching behaviours of plasmachemical processes which result in changes to GaAs surface roughness. This indicates that at appropriate set of experimental parameters (i.e., exposure time, feeding voltage, illumination intensity, discharge gap and gas pressure) the formation of very smooth cathode surface is induced by plasma etching of GaAs plate. Moreover, this very smooth semiconductor surface also enhanced the homogeneity of DLE and consequently the spatial resolution and image contrast in a PGDS could be improved considerably. It has been found while the quality of the GaAs surface in a PGDS can be assessed by the fractal dimension estimation, the effect of plasmachemical processes for optimal and arbitrary experimental parameters are separately determined using fractal concept. The results obtained in this work suggest that a PGDS can be an efficient, alternative plasma source for general surface processing, because they can provide nonthermal discharges also near atmospheric pressures and thereby eliminate the need of costly vacuum systems.

[1] *V. Malhotra, C.W. Wilmsen.* In: Holloway PH, McGuire GE, editors. Passivation of GaAs and InP in Handbook of Compound Semiconductors, Noyes Publications: New Jersey, 1995, pp.328-69.
[2] *P.B. Vigneron, F. Joint, N. Isac, R. Colombelli, E. Herth.* Microelectronic Engineering. 2018, 202, 42.
[3] *V.R. Agarwal, D.S. Rawal* and *H.P. Vyas.* J. Electrochem. 2005, Soc., 152, 567.
[4] *Y.W. Chen, B.S. Doi, G.I. Ng, K. Radhakrishnan and C.L Tan.* J. Vac. Sci. Technol., 2000, *B*, 18, 2509.
[5] *M.A. Liebermann* and *A.J. Lichtenberg.* Principles of Plasma Discharges and Materials Processing.,1994, Wiley, New York.
[6] *J. Rutkowski, W. Fourcault, F. Bertrand, U. Rossini, S. Gétin, S. Le Calvez, T. Jager, E. Herth, C. Gorecki, M. Le Prado, J.M. Léger, S. Morales.* Sensors Actuators A Phys., 2014, 216, 386.
[7] *R. Schwarz and J.G. Salge*. in Proceedings of the 11th International Symposium on Plasma Chemistry, edited by J. Harry., Loughborough, Le-icestershire, England, 1993.
[8] *M. Karlsson, F. Nikolajeff.* 2002, Appl. Opt. 41, 902, 1539.
[9] *H. Willebrand, Y.A. Astrov, L. Portsel, S. Teperick, T. Gauselmann.* Infrared Phys. & Technol.,1995, 36 (4), 809.
[10] *B.G. Salamov, A.Kh. Zeinally, N.N. Lebedeva* and *L.G. Paritskii.,* 1991, J. Photogr. Sci., 39, 114.
[11] *Y. Sadiq, K. Aktas, S. Acar* and *B.G. Salamov. Superlattices Microstruct.*, 2010, 47, 648.
[12] *F. Hasegawa, M. Onomura, C. Mogi* and *Y. Nannichi.*, Solid-State Electron, 1988, 31, 223
[13] *Ch. Radehaus, T. Dirksmeyer, H. Willebrand* and *H-G. Purwins.* Phys. Lett. 1987, A 125 92
[14] *H.Willebrand, T. Hünteler, F. Niedernostheide, R. Dohmen* and *H-G. Purwins.* Phys.Rev. 1992, *A* 45 8766
[15] *S. Ozturk Koç, S. Galioglu, B. Akata, E. Koç, B.G. Salamov.* J. Electronic Materials., 2018, 47, (5), 2791.
[16] *H. (Yücel) Kurt, E. Kurt, B.G. Salamov.* Imaging. Sci. J., 2001, 49**,** 205.
[17] *K. Germanova, V. Donchev, Ch. Chardalov and L. Nikolov.* J.Phys.D, 1987, 20, 1507.
[18] *K. Koseoglu, B.G. Salamov.* Plasma Process. Polym. 2016, 13, №3, 355.
[19] *K. Koseoglu, M. Özer, B.G. Salamov.* IEEE Transactions on Plasma Science., 2015, 43, №10, 3576.
[20] *L.V. Belyakov, A.B. Mageramov* and *L.G. Paritskii.* Sov. Phys. Semicond., 1978, 12, 6, 739.
[21] *K. Aktas, S. Acar, B.G. Salamov.* Plasma Sources Sci. Technol. 2011, 20, 045010.
[22] *T. Ohmi, M. Miyashita* and *T. Imaoka.* Proceeding of the Microcontamination Meeting, Canon Communications, San Jose, CA, 1991, pp.491.
[23] *M. Heyns, C. Hasenack, R. De Keersmaecker and R. Falster, J. Ruzyllo* and *R.E. Novak* (eds.). Proc. of the 1st Int. Symp. on Cleaning

Technology in Semiconductor Device Manufacturing, PV 90-9, Electrochemical Society, Pennington, NJ, 1990, p.293.

[24] *S.W. Robey*. Phys. Rev. 2002, B, 65, 115

[25] *Z. Falkenstein* and *J. Cogan.* J. Appl. Phys., 1997, 82 (12), 6273.

[26] *G. Xu, L. Li, N. Isac, Y. Halioua, A. Giles Davies, E.H. Linfield, R. Colombelli.* Appl. Phys. Lett., 2014,104, 091112.

[27] *Y. Sadiq, M. Ozer, B.G. Salamov.* J. Phys. D: Appl. Phys. 2008, 41, 045204.

[28] *Ma S.* and *McVittie J.P*. J. Vac. Sci. Technol., 1996, *B*, 14, 566.

[29] *S. Fang* and *McVittie J.P*. IEEE Trans. Electron Devices, 1994, 41, 1034.

[30] *Z. Synowiec.* Vacuum, 2001, 63, 487.

[31] *Li X W, J.F. Tian, Y. Kang* and *Z.G. Wang.* Scripta Metall. & Mater., 1995,33,5, 803.